



<http://www.diva-portal.org>

Postprint

This is the accepted version of a paper published in . This paper has been peer-reviewed but does not include the final publisher proof-corrections or journal pagination.

Citation for the original published paper (version of record):

Asan, N B., Carlos, P P., Redzwan, S., Noreland, D., Hassan, E. et al. (2017)  
Data Packet Transmission through Fat Tissue for Wireless Intra-Body Networks.  
*IEEE Journal of Electromagnetics, RF and Microwaves in Medicine and Biology*  
<https://doi.org/10.1109/JERM.2017.2766561>

Access to the published version may require subscription.

N.B. When citing this work, cite the original published paper.

Permanent link to this version:

<http://urn.kb.se/resolve?urn=urn:nbn:se:uu:diva-335351>

# Data Packet Transmission through Fat Tissue for Wireless Intra-Body Networks

Noor Badariah Asan, *Student Member, IEEE*, Carlos Pérez Penichet, Syaiful Redzwan, *Student Member, IEEE*, Daniel Noreland, Emadeldeen Hassan, Anders Rydberg, *Member, IEEE*, Taco J. Blokhuis, Thiemo Voigt, *Member, IEEE*, and Robin Augustine, *Member, IEEE*

**Abstract:** This work explores high data rate microwave communication through fat tissue in order to address the wide bandwidth requirements of intra-body area networks. We have designed and carried out experiments on an IEEE 802.15.4 based WBAN prototype by measuring the performance of the fat tissue channel in terms of data packet reception with respect to tissue length and power transmission. This paper proposes and demonstrates a high data rate communication channel through fat tissue using phantom and *ex-vivo* environments. Here, we achieve a data packet reception of approximately 96 % in both environments. The results also show that the received signal strength drops by  $\sim 1$  dBm per 10 mm in phantom and  $\sim 2$  dBm per 10 mm in *ex-vivo*. The phantom and *ex-vivo* experimentations validated our approach for high data rate communication through fat tissue for intra-body network applications. The proposed method opens up new opportunities for further research in fat channel communication. This study will contribute to the successful development of high bandwidth wireless intra-body networks that support high data rate implanted, ingested, injected, or worn devices.

**Keywords** — Intra-body communication, microwave, channel characterization, data packet, Software Defined Radio, GNU Radio, *ex-vivo*, phantom.

## I. INTRODUCTION<sup>1</sup>

**I**NTRA-BODY Area Networks (Intra-BANs) is a key technology that uses the human body as a communication channel to allow implanted devices to exchange information between each other. Recently, there has been a growing interest in biomedical science and networking technology. Many researchers have extensively studied wireless medical devices that can be implanted [1–3], ingested [4–5], injected [6–7] or worn [8–9] as well as communication between such devices. This cross-fertilization improves various applications such as drug infusing and dispensing, artificial heart and heart assist devices, implantable sensors, and control of other artificial organs [10].

This paper is an expanded paper from the IEEE IMBioC 2017, Gothenburg, Sweden. This work was supported by Ministry of Higher Education Malaysia, Eurostars project under Grant E-9655-COMFORT, Swedish Vinnova project under Grant BDAS (2015-04159) and Reliable, interoperable and secure communication for body network (2017-03568), and a strategic collaborative eScience program by Swedish Research Council under Grant eSENCE.

<sup>1,2</sup>Noor Badariah Asan, <sup>1</sup>Syaiful Redzwan, <sup>1</sup>Anders Rydberg and <sup>1</sup>Robin Augustine are with the <sup>1</sup>Microwaves in Medical Engineering, Microwave Group, Department of Engineering Sciences, Uppsala University, Uppsala, Sweden, and with the <sup>2</sup>Faculty of Electronic and Computer Engineering, Universiti Teknikal Malaysia Melaka, Melaka, Malaysia (e-mail: noorbadariah.asan@angstrom.uu.se, syaiful.redzwan@angstrom.uu.se; anders.rydberg@angstrom.uu.se; robin.augustine@angstrom.uu.se).

Carlos Pérez Penichet and Thiemo Voigt are with the Department of Information Technology, Division of Computer Systems, Uppsala University, Uppsala, Sweden (carlos.penichet@it.uu.se; thiemo@sics.se).

<sup>3</sup>Daniel Noreland and <sup>3,4</sup>Emadeldeen Hassan are with the <sup>3</sup>Department of Computing Science, Umeå University, Umeå, Sweden and <sup>4</sup>Department of Electronics and Electrical Communications, Menoufia University, 32952- Menouf, Egypt. (noreland@cs.umu.se; emad@cs.umu.se).

Taco J. Blokhuis is with the Department of Surgery, Maastricht University Medical Center+, P. Debyealaan 25, 6229 HX Maastricht, The Netherlands (taco.blokhuis@mumc.nl).

In healthcare monitoring applications, sensor nodes are placed inside the human body and need to communicate with each other. Besides, many applications that require high data rate communication such as cardiac pacemakers [11], implantable cardioverter/defibrillators (ICD) [12] and neuroprosthetics [13] devices now exist in the market. Due to the growth of sensors that require high data rate, the demand of high bandwidth has increased which provides opportunities for researchers to investigate new research areas.

Generally, three different techniques have been used to propagate a signal onto the human body: Galvanic coupling [14–18], capacitive coupling [17–22], and RF links [23–29]. Usually higher frequencies are not suitable for intra-body communication due to the lossy nature of biological tissues [30,31]. On the other hand, low frequencies cannot support high bandwidth. For this reason, researchers have been investigating the possibilities of using different human tissue channels to support low loss microwaves communication. Microwaves are attenuated by the human body due to the high dielectric losses of skin and muscle tissues. For this work, however, we propose the communication through the fat tissue, which offers lower losses for microwave propagation compared to other tissues. We have previously demonstrated the feasibility of using fat tissue as a low loss microwave transmission channel for intra-body communication [32–33]. But, for a successful communication scenario, real data has to be transferred through a given channel. To the best of our knowledge, this work presents the first comprehensive data packet transmission study that uses the fat tissue as a communication channel. Table I summarizes some state of the art intra-body / on-body communication scenarios.

TABLE I  
STATE OF THE ART INTRA-BODY / ON-BODY COMMUNICATION

Work	Technique	Frequency	Transmission coefficient, $S_{21}$	Path Loss
[17]	Galvanic coupling	40 kHz	-	~ -39 dB (d=10 cm)
[18]	Galvanic coupling	100 kHz	-	~ -47 dB (d=10 cm)
[30]	Galvanic coupling	100 MHz	~ -37 dB (d=15 cm)	-
[17,18]	Capacitive coupling	100 MHz	-	~ -27 dB (d=15 cm)
[20]	Capacitive coupling	10 MHz	~ -18 dB d=16 cm	-
[21]	Capacitive coupling	26 MHz	~ -32 dB (d=30 cm)	-
[24]	RF	403.5 MHz	-	~ 54 dB (d=10 cm)
[25]	RF	915 MHz	-51.4 dB (d=0.5 cm)	-
[26]	RF	1 GHz	~ -56 dB (d=0.75 cm)	-

\*d = transmission distance.

In this work, we conduct extensive studies to demonstrate the possibility of sending data packets through the fat tissue. We present a microwave propagation study in the R-band (frequency range of 1.7 GHz - 2.6 GHz), that overlaps with the Industrial, Scientific, and Medical (ISM) radio frequency band (1.8 GHz and 2.4 GHz) for implant communications. In this work, we develop a model and perform channel measurements to observe the performance of the data packet transmission in a three-layer homogeneous phantom and *ex-vivo* porcine belly tissue, consisting of skin, fat, and muscle tissue.

The remainder of the paper is organized as follows: In Section II, we describe the materials and the methodology of channel propagation, received signal strength and data packet reception. Based on this, the whole experimental setup for both measurements are presented. The results and discussion is given in Section III. Finally, the paper ends with the conclusion.

## II. MATERIALS AND METHODS

### A. Characterization of Propagation Channel

Homogeneous three-layer tissues, consisting of skin, fat, and muscle were used to study the wave propagation and to investigate the dependence of the transmission channel quality on the thickness and the length of the fat tissue. The simulation model was designed in Computer Simulation Technology – CST Microwave Studio Package and has been processed using a time domain solver (<http://www.cst.com>). A three-layer model was prepared and simulated at the R-band frequency range of 1.7 GHz to 2.6 GHz. Fig. 1 demonstrates the concept of using the fat tissue as a communication channel. A transmitter (TX) launches an electromagnetic signal into the fat tissue. The microwave signal travels through the fat tissue and is received at a receiver (RX) located on the opposite side of the fat tissue. The reflection coefficient ( $S_{11}$ ) and

transmission coefficient ( $S_{21}$ ) can be recorded at the transmitter and the receiver, respectively.

Moreover, in order to scrutinize the dependence of the transmission channel quality on the thickness and the length of the fat tissue, we designed two simulation models, namely Model A and Model B. Referring to Fig. 2(a), Model A consists of three-layer tissues and is designed with a dimension of 50 mm  $\times$  100 mm (width (W)  $\times$  length (L)). Further, we vary the thickness of the fat ( $T_F$ ) from 10 mm to 35 mm and the muscle thickness ( $T_M$ ) from 20 mm to 45 mm while we fix the skin thickness ( $T_S$ ) at 2 mm to study the behavior of the scattering parameters (S-parameters) according to the thickness variations. We use the bio-tissue models for the skin, the fat, and the muscle from the CST material library to characterize the tissues in the two models.

For Model B as shown in Fig. 2(b), we replace the theoretical CST waveguide ports with two realistic, custom-made waveguide probes. In Model B, the experiments were carried out in two different environments; (1) phantom equivalent tissue and (2) *ex-vivo* tissue. This is to provide the performance benchmark in a realistic environment, which is the human tissue. From a porcine tissue obtained from a local slaughter house, we extracted with the skin, fat, and muscle. For the entire study in Model B, the model consists of 2 mm, 25 mm, and 30 mm thick skin, fat, and muscle, respectively. We vary the signal transmission distance from 20 mm to 100 mm, with a 20 mm step, for the phantom and the *ex-vivo* setups. These distances were chosen based on the distance between several vital organs such as liver–kidney, pancreas–kidney, and liver–heart and also from the experimental models adopted in previous studies [14, 25]. To prove that the fat tissue is a good communication channel compared to the muscle tissue, we compare the results of using the fat tissue as a communication channel against the results obtained when the muscle tissue is used. For both Model A and Model B, we aligned the probe with the muscle layer and repeat the same experiments as for the fat layer.

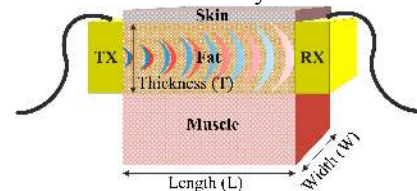


Fig. 1. The concept of channel propagation through the fat tissue.

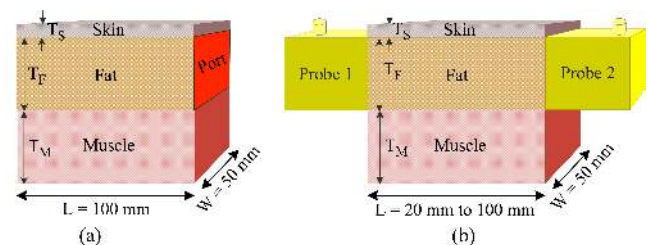


Fig. 2. Two models for the skin-fat-muscle channel.

(a) Model A: Using a theoretical waveguide port.

(b) Model B: Using a realistic waveguide probe.

Fig. 3 shows the configuration of the probe that we use to launch the microwave signal into the tissue. Each probe consists of a 50 mm × 70 mm × 25 mm rectangular waveguide section, matched to a 50-Ohm coaxial-cable through a topology optimized planar antenna (TOPA) that vertically resides at the center of the waveguide section. The copper distribution over the antenna part is determined by using a recently proposed gradient-based topology optimization method that can efficiently handle tens of thousands of designs variables [34].

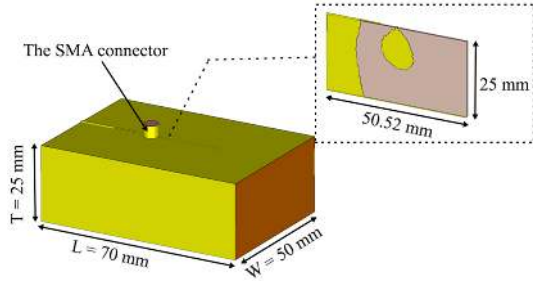


Fig. 3. The configuration of the waveguide probe.

Fig. 4 shows the fabricated probe. The two copper parts comprising the antenna are a radiating lump, connected to the SMA connector, and a back reflector connected to the rear end of the waveguide section to provide proper matching [34]. The prototype antenna is developed using photolithography on a 0.762 mm thick Rogers-3203 dielectric substrate with relative permittivity ( $\epsilon'$ ) of 3.02, loss tangent ( $\tan \delta$ ) of 0.016, and a total dimension of 25 mm × 50.52 mm (width × length). The prototype consists of four parts: The planar antenna, the rectangular waveguide section, the fat-equivalent tissue filling the interior of the waveguide section, and the subminiature version A (SMA) connector. The probe-to-probe measurements were taken to set the baseline and to assess the operating frequency [33].

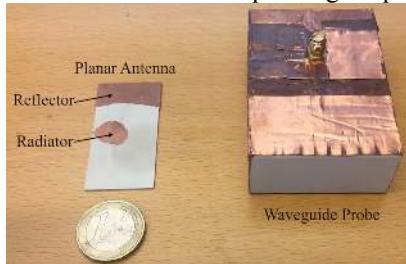


Fig. 4. The topology optimized planar antenna and the rectangular waveguide section [34].

In this pilot study, slight variations that can happen in *ex-vivo* tissue properties are not taken into consideration during measurements. Fig. 5 shows the setup used in characterizing the propagation channel. The dielectric properties for phantom and the *ex-vivo* tissues were measured using an Agilent dielectric slim probe kit (Series number: 85070E) [35]. For each tissue, three measurements were performed in three different locations, and the average value for each tissue was taken. The dielectric properties of the tissue-equivalent phantom and the *ex-vivo* tissues are listed in Table II.

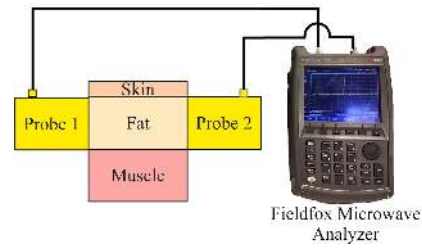


Fig. 5. The setup for the propagation channel measurement.

TABLE II  
COMPARISON OF DIELECTRIC PROPERTIES ( $\epsilon'$  AND  $\tan \delta$ ) OF THE PHANTOM, *EX-VIVO*, AND HUMAN AT 2.0 GHz [36]

Tissue	Parameter	Material / Environment		
		Phantom	<i>Ex-vivo</i>	Human
Skin	Relative permittivity	38.182	34.839	38.570
	Loss tangent	0.203	0.343	0.295
Fat	Relative permittivity	5.038	4.096	5.328
	Loss tangent	0.010	0.202	0.145
Muscle	Relative permittivity	56.114	48.855	53.290
	Loss tangent	0.201	0.317	0.245

### B. Setup Requirement for Data Packet Study

We used the IEEE 802.15.4 standard for Low-Power Wireless Personal Area Networks (LP-WPANs) [37] physical layer and medium access sub-layer protocols. Specifically, this standard provides specifications for different license-free ISM bands. For the 2.4 GHz ISM band, the standard defines a physical layer with 16 channels spaced every 5 MHz. The data is modulated with Offset Quadrature Phase Shift Keying (O-QPSK) modulation (with half-sine pulse shaping) and transmitted at a resulting data rate of 250 kbps.

In order to increase the robustness of the low-power transmissions, the IEEE 802.15.4 standard uses Direct Sequence Spread Spectrum (DSSS). Each 4-bit data symbol is mapped to a 32-bit long pseudo-random chip sequence, which in turn is modulated using O-QPSK. Since each O-QPSK symbol takes on one of four possible phases [38], it encodes two chips per symbol. The resulting modulated signal has a bandwidth of 2 MHz. The fat channel has an optimal transmission band at 2.0 GHz as can be seen in the Section III. For this reason, we have focused our data packet experiments at 2.0 GHz. Since no standard-compliant 802.15.4 transceiver can operate at 2.0 GHz, we resorted to a software-defined 802.15.4 transceiver.

Our data transmission experiments were performed with the GNU Radio-based 802.15.4 transceiver by Bloessel et al. [39] using a USRP B200 Software Defined Radio (SDR). GNU Radio is an open source development toolkit to implement software-defined radios in a computer. GNU radio provides various signal processing blocks and other tools that, when paired with the appropriate hardware, can be used to implement software radios.

### C. Data packet reception and received signal strength

Two separate experimental setups were used to characterize the data packet reception and received signal strength measurements. The experiments were carried out both in phantom and *ex-vivo* environments.

### Received Signal Strength

Fig. 6 shows the experimental setup for measuring the received signal strength. The RF TX from the SDR was connected to the Probe 1. The signal propagates through the fat tissue channel and is received at Probe 2. The signal strength is measured with a FieldFox Handheld Microwave Analyzer (Series number: N9918A) [40]. During the measurement, we measure the power received at Probe 2. We obtained the received signal strength by observing the output power at each distance.



Fig. 6. Received signal strength measurement setup.

### Data packet reception

Fig. 7 shows the experimental setup for both phantom and *ex-vivo* data packet transmission. In this configuration, the USRP device is connected to a host PC via USB. In order to measure the performance of the proposed concept, Probe 1 was connected to the Radio Frequency transmitter (RF TX) port and Probe 2 was connected to the Radio Frequency receiver (RF RX) port. The SDR transmits the packets at 2.0 GHz with 250 kbit/s. For each distance, five measurements were performed with 1000 data packets transmitted for each measurement. The packets were received and analyzed using the Wireshark software. The percentage of data packets received with probe-to-probe measurement is used as a reference. Six different input powers (from -25 dBm to 0 dBm) were demonstrated to identify the optimum power for data transmission. Fig. 8 shows the experimental setup of the two environments. Both experiments have been done in the laboratory at 22 °C (71.6 °F) with 36% relative humidity. A surgical scalpel was used to cut the tissues into their respective dimensions.

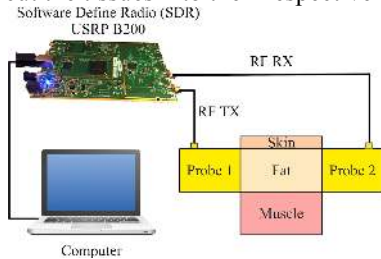


Fig. 7. Experimental setup for packets measurement setups.



Fig. 8. Experimentation setup in (a) Phantom and (b) *Ex-vivo* environments consisting of skin, fat, and muscle layer.

## III. RESULTS AND DISCUSSION

### A. Characterization of the Propagation Channel

#### The dependence of the transmission channel quality on tissue thickness

Fig. 9 and Fig. 10 show the effect on the transmission channel quality by varying the thickness of fat and muscle tissues when the waveguide ports are aligned with the fat layer and the muscle layer, respectively.

To study the impact of fat thickness, we fix the skin and muscle thicknesses at 2 mm and 30 mm respectively, while varying the fat thickness by 5 mm from 10 mm to 35 mm. As shown in Fig. 9 (a), the transmission coefficient ( $S_{21}$ ) is improved when the fat tissue thickness increases until 25 mm and it does not improve much when the thickness is increased further. Fig. 9 (b) shows the result under the condition that the muscle tissue thickness is varied by 5 mm from 20 mm to 45 mm, respectively, while the skin and fat thicknesses were fixed at 2 mm and 25 mm. The simulation results show that both amplitudes of  $S_{11}$  and  $S_{21}$  remained almost constant. Therefore, the signal transmission quality is not affected by the muscle thickness.

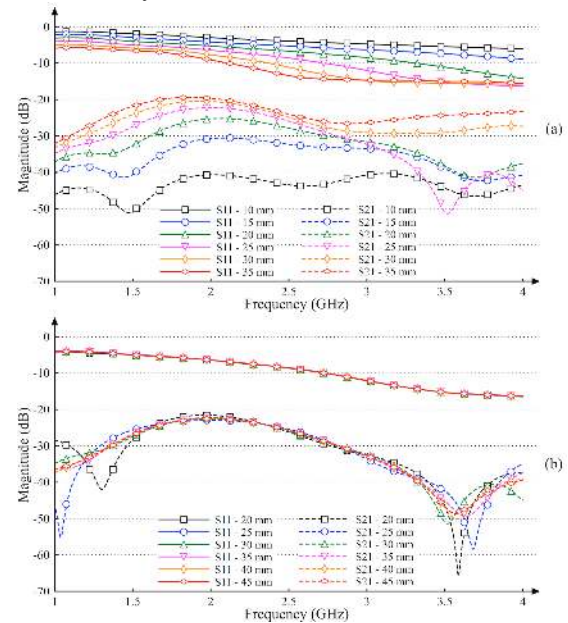


Fig. 9. The effect of the fat tissue thickness on  $S_{11}$  and  $S_{21}$  from the simulation (a) skin = 2 mm, fat = 10 mm to 35 mm, muscle = 30 mm, (b) skin = 2 mm, fat = 25 mm, muscle = 20 mm to 45 mm. Waveguide port aligned with the fat layer.

Fig. 10 (a) shows the S-parameters simulation results obtained for waveguide ports aligned with the muscle layer while the thickness of fat layer was varied from 10 mm to 35 mm by 5 mm. In Fig. 10 (b), the muscle layer thickness was varied from 20 mm to 45 mm by 5 mm while keeping fat layer thickness fixed at 25 mm. The waveguide ports are aligned with the muscle layer for S-parameters simulation. Fig. 10 (a) and Fig. 10 (b) show that when the waveguide ports are aligned to the muscle layer, there is no substantial variation in the S-parameters with respect to the change in the fat or muscle tissue thickness. Compare the  $S_{21}$  from

Fig. 9 with Fig. 10 at 2.0 GHz, we infer that the magnitude is 10 dB better in the case of waveguide ports aligned with the fat layer than with the muscle layer.

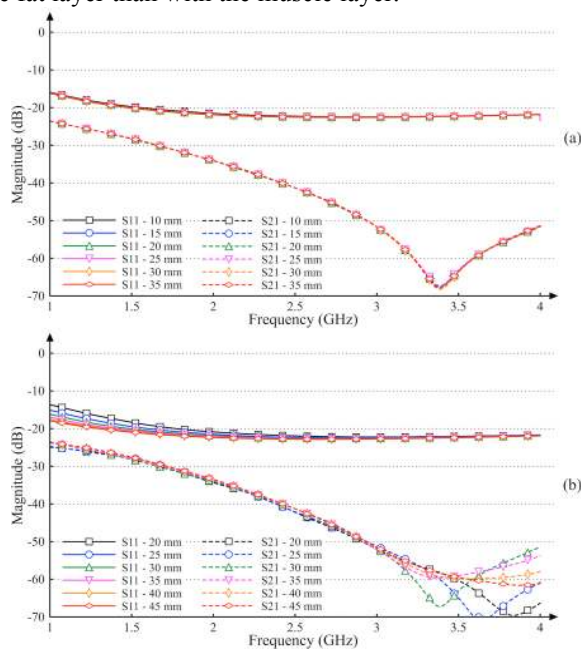


Fig. 10. The effect of the fat tissue thickness on  $S_{11}$  and  $S_{21}$  from the simulation (a) skin = 2 mm, fat = 10 mm to 35 mm, muscle = 30 mm, (b) skin = 2 mm, fat = 25, muscle = 20 mm to 45 mm. Waveguide port aligned with the muscle layer.

### Comparison with respect to the tissue length

In order to investigate the influence of the tissue length between the two probes, the corresponding measurement and simulations were carried out. To compare the microwave coupling through the muscle tissue against the coupling through the fat tissue, we repeated the measurement with the probes aligned to the muscle layer. Fig. 11 shows the reflection coefficient ( $S_{11}$ ) comparison between simulation and measurement results. We vary the channel length from 20 mm to 100 mm, with a 20 mm step, for the phantom and the *ex-vivo* experiments. Fig. 11 (a) and Fig. 11 (b) show the  $S_{11}$  results when the waveguide ports are aligned with the fat layer and the muscle layer, respectively. The slight disagreement in resonant frequency may have been caused by the positioning of the probes within the three-layer tissues, the variation in dielectric properties, and the losses of the prototype during fabrication. Since our primary focus is on lateral intra-body communication,  $S_{21}$  is given special attention.

Fig. 12 shows the  $S_{21}$  comparison between simulation and measurement results corresponding to the signal transmission distance varied by 20 mm from 20 mm to 100 mm for phantom and *ex-vivo* environment. Fig. 12 (a) and Fig. 12 (b) show the  $S_{21}$  results when the waveguide ports are aligned with the fat layer and the muscle layer, respectively. It can be seen that the simulation results at 2.0 GHz are comparable with the measurement results. According to the results shown in Fig. 12 (a), both the simulation and the measurement show a decrease in the amplitude by  $\sim 2$  dB per 20 mm for phantom and  $\sim 4$  dB per

20 mm for *ex-vivo* as the distance between the two probes increases from 20 mm to 100 mm.

Table III shows the  $S_{21}$  data extracted from the simulation and measurement at 2.0 GHz. From Table I and Table III, we infer that our proposed fat channel model facilitates better signal coupling compared to existing techniques. Fig. 12 (b) shows that the transmission loss (dB) in the muscle layer is more than two-fold of the transmission loss (dB) through the fat layer as in Fig 12 (a). From Fig. 12, we can conclude that, the fat layer is a better communication channel than the muscle layer.

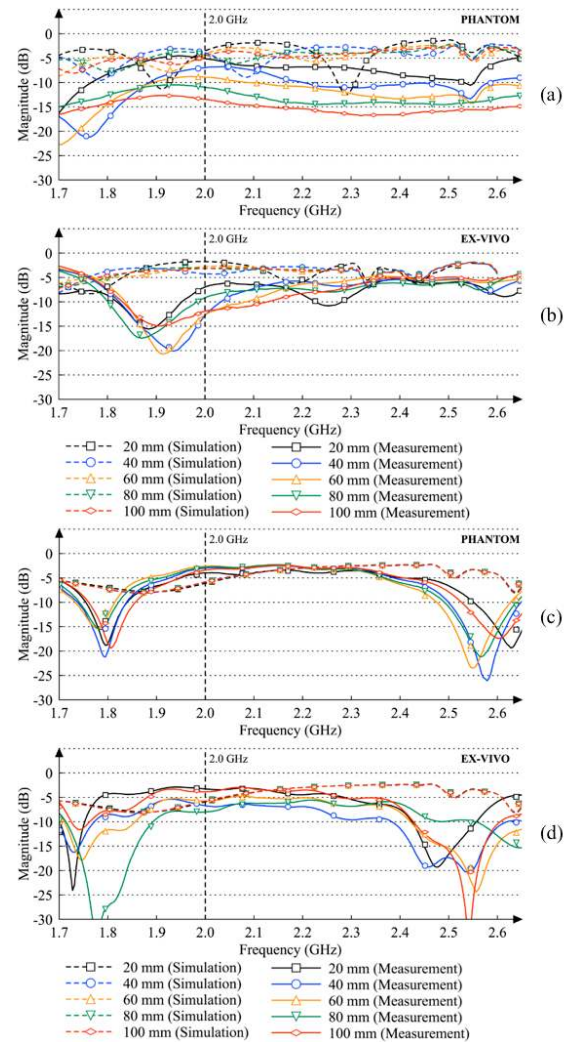


Fig. 11. Reflection coefficient ( $S_{11}$ ) comparison between measurement and simulation results corresponding to the signal transmission distances for phantom and *ex-vivo*. (a) and (b): Probe aligned with the fat layer, (c) and (d): Probe aligned with the muscle layer.

### B. Received signal strength and data packet reception

#### Received Signal Strength

In this sub-section, we investigate the minimum transmission power required for a reliable communication. We carry out the experiment to observe the received signal strength (dBm). For the phantom and the *ex-vivo* tissues, we vary the length of the fat-channel from 10 mm to 100 mm with a 10 mm step. The probe-to-probe results determine the baseline of the performance of the communication link.

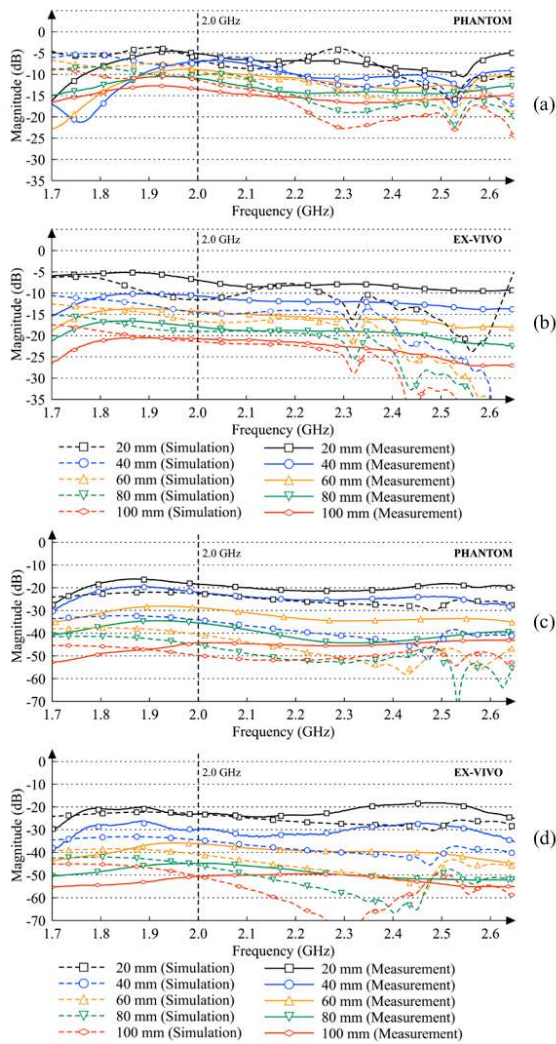


Fig. 12. Transmission coefficient ( $S_{21}$ ) comparison between measurement and simulation results corresponding to the signal transmission distances for phantom and *ex-vivo*. (a) and (b): Probe aligned with the fat layer, (c) and (d): Probe aligned with the muscle layer.

TABLE III  
TRANSMISSION COEFFICIENT ( $S_{21}$ ) DATA AT 2 GHz FOR SIMULATION AND MEASUREMENT (PROBE ALIGNED WITH THE FAT LAYER)

Distance (mm)	Simulation		Measurement	
	Phantom $S_{21}$ (dB)	<i>Ex-vivo</i> $S_{21}$ (dB)	Phantom $S_{21}$ (dB)	<i>Ex-vivo</i> $S_{21}$ (dB)
20	-6.51	-11.57	-5.18	-7.06
40	-7.22	-14.60	-6.88	-10.70
60	-9.16	-16.58	-8.94	-14.33
80	-10.18	-19.03	-11.04	-17.99
100	-11.42	-21.40	-13.51	-20.74

We vary the transmission power from -25 dBm to 0 dBm for both environments. The transmission efficiency is defined as the ratio of the received signal strength at the receiver to the transmission power at the transmitter. The solid and dashed lines in Fig. 13 indicate measurements using the three-layer tissue-equivalent phantom and *ex-vivo* tissues, respectively. For both environments, the transmission efficiency is decreased as the distance between the transmitter and receiver is increased. This is because; the coupling between the transmitter and receiver is reduced

depending on the distance between them. At 2.0 GHz, the signal strength decreases with  $\sim 1$  dBm per 10 mm in phantom, while  $\sim 2$  dBm per 10 mm in *ex-vivo*. The path loss is defined as the ratio of power transmitted ( $P_{tr}$ ) to power received ( $P_{rec}$ ) [41].

$$PL_{dB} = (P_{tr} / P_{rec}) = -10 \log_{10} |S_{21}|^2 = -|S_{21}|_{dB} \quad (1)$$

The received power measurement with respect to the three-layer tissue lateral distance is shown in Fig. 13. The probe-to-probe power received is considered as a default path loss of the transceiver system. Therefore, for calculating the channel path loss, the default loss is subtracted from the total path loss for a given channel length. Thus, the average path loss for 10 mm of three-layer phantom and *ex-vivo* tissues calculated using (1) are 1 dB and 2 dB, respectively. Therefore, our proposed fat channel offers low path loss for intra-body communication applications.

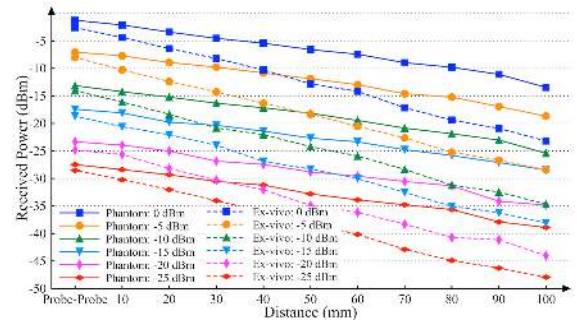


Fig. 13. The received power through the phantom and the *ex-vivo* fat-channels versus the channel length.

#### Data packet reception

We carry out the experiment to observe the percentage of data packet reception with the distance variation. We vary the distance from 20 mm to 100 mm, with a 20 mm step, both for the phantom and the *ex-vivo* tissues. Fig. 14 shows the percentage of packets received for the phantom and the *ex-vivo* at different transmission powers. The error bars show the minimum and the maximum value for each distance. From the bar chart, the average packet reception is approximately 96 % for both phantom and *ex-vivo* experiments. For the phantom, at high transmission power (0 dBm), a substantial increase of reflection occurs at the receiver probe degrading the ongoing transmissions and preventing future data packet reception. Meanwhile, in the *ex-vivo* context, the inherent losses in biological tissue diminish backward reflection and facilitate higher data packet reception. Considering the limitation of SDR, the minimum power level that we have used is -25 dBm even though good packet reception might be possible also at lower transmission powers. Due to the device constraints, currently we are not able to estimate the lower power limit for reliable data packet transmission. Our results show that low transmission power is sufficient. Furthermore, reducing the transmission power will reduce interference on other nodes and may enhance both the overall network throughput and energy consumption [42].

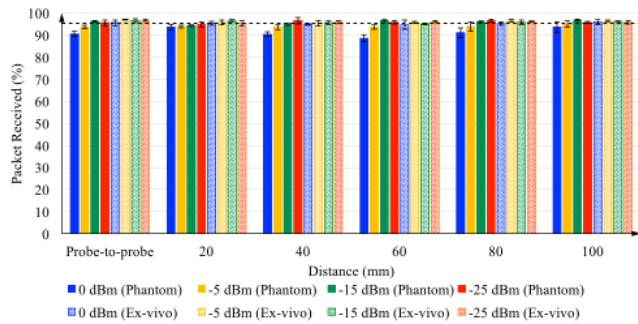


Fig. 14. Percentage of packets received for phantom and *ex-vivo* environments at different transmission power.

As the applications for which the communication model was developed do not require long distances, the range of distance between the transmitter and the receiver was set to 10 mm to 100 mm in our experiments. The measurements presented here demonstrate that reliable data transmission is possible through the porcine fat tissue. The measurements show that the transmission power and receiver sensitivity are important factors for the performance of a communication system. Therefore, there should be an optimal power level for successful data packet transfer and reduction of any possible signal interference that corrupts data packet reception. If the signal is too weak, the receiver cannot correctly receive the transmitted information.

#### IV. CONCLUSION

In this paper, a communication link using a three-layer phantom, *ex-vivo* tissue is simulated and measured. The efficiencies at 2.0 GHz between the transmitter and the receiver were investigated. We designed a high data rate microwave communication link through fat tissue and experimentally demonstrated the performance of the proposed communication using phantom and *ex-vivo* setups. Specifically, we reached data reception up to 96 % for both phantom and *ex-vivo* communication, which may enable intra-body applications requiring high sampling rates such as neural data recording and wireless endoscopic pills. The results show that the signal strength drops by  $\sim 1$  dBm per 10 mm in phantom and  $\sim 2$  dBm per 10 mm in *ex-vivo*. The phantom and *ex-vivo* experimentations validated our approach for high data rate communication through fat tissue for intra-body network applications.

To the best of our knowledge, the development of microwave communication through fat tissue is completely original since no similar reports have been found in the literature. Therefore, this work will be beneficial in establishing communication in intra-body area networks. Future work includes the development of an analytical model for the proposed fat channel. The different modulation schemes and IEEE standards in wireless body area networks (WBANs) will be investigated to improve the performance and the efficiency of the system. In the near future, we will also study the effect of embedded muscle, blood vessels, or any other physical disturbances in the fat channel such as body posture, the influence of body

dynamics, and the effect of surrounding environment. Since the properties of biological porcine fat tissue are similar to the human fat tissue, we hope that we will be able to demonstrate reliable microwave transmission through human tissue in the future. Ethical approval to conduct clinical trials is under-way. Using human body tissues as communication channel is attractive for a range of futuristic medical applications. This work also has potential application in man-machine interfaces.

#### REFERENCES

- [1] P. Cong, W. H. Ko and D. J. Young, "Wireless Batteryless Implantable Blood Pressure Monitoring Microsystem for Small Laboratory Animals," in *IEEE Sensors Journal*, vol. 10, no. 2, pp. 243–254, Feb. 2010.
- [2] S. M. Asif *et al.*, "Design and In Vivo Test of a Batteryless and Fully Wireless Implantable Asynchronous Pacing System," in *IEEE Transactions on Biomedical Engineering*, vol. 63, no. 5, pp. 1070–1081, May 2016.
- [3] H. W. Chiu *et al.*, "Pain Control on Demand Based on Pulsed Radio-Frequency Stimulation of the Dorsal Root Ganglion Using a Batteryless Implantable CMOS SoC," in *IEEE Transactions on Biomedical Circuits and Systems*, vol. 4, no. 6, pp. 350–359, Dec. 2010.
- [4] J. Thoné, S. Radiom, D. Turgis, R. Carta, G. Gielen, R. Puers, "Design of a 2Mbps FSK near-field transmitter for wireless capsule endoscopy," in *Sensors and Actuators A: Physical*, vol. 156, no. 1, pp. 43–48, Nov. 2009.
- [5] S. P. Woods and T. G. Constantinou, "Wireless Capsule Endoscope for Targeted Drug Delivery: Mechanics and Design Considerations," in *IEEE Transactions on Biomedical Engineering*, vol. 60, no. 4, pp. 945–953, Apr. 2013.
- [6] X. Li *et al.*, "The injectable neurostimulator: An emerging therapeutic device," in *Trends in Biotechnology*, vol. 33, no. 7, pp. 388–394, Jul. 2015.
- [7] E. Johannessen *et al.*, "Toward an injectable continuous osmotic glucose sensor," in *Journal of Diabetes Science and Technology*, vol. 4, no. 4, pp. 882–892, Jul. 2010.
- [8] Z. H. Jiang, D. E. Brocker, P. E. Sieber and D. H. Werner, "A Compact, Low-Profile Metasurface-Enabled Antenna for Wearable Medical Body-Area Network Devices," in *IEEE Transactions on Antennas and Propagation*, vol. 62, no. 8, pp. 4021–4030, Aug. 2014.
- [9] T. Liang and Y. J. Yuan, "Wearable Medical Monitoring Systems Based on Wireless Networks: A Review," in *IEEE Sensors Journal*, vol. 16, no. 23, pp. 8186–8199, Dec. 1, 2016.
- [10] Didier Sagan, "RF Integrated Circuits for Medical Applications", Available at <http://stf.ucsd.edu/presentations/2007-08%20STF%20-%20Zarlink%20ULP%20transceivers.pdf>, accessed July 2017.
- [11] C. Guo *et al.*, "An inductive wireless telemetry circuit with OOK modulation for implantable cardiac pacemakers," in *2015 IEEE 11th International Conference on ASIC (ASICON)*, Chengdu, 2015, pp. 1–4.
- [12] K. Rohit, and M. Saeed, "Implantable Cardioverter-Defibrillators: Indications and Unresolved Issues," in *Texas Heart Institute Journal*, vol. 39, no. 3, pp. 335–341, 2012.
- [13] D. Borton *et al.*, "Developing implantable neuroprosthetics: A new model in pig," *2011 Annual International Conference of the IEEE Engineering in Medicine and Biology Society*, Boston, MA, 2011, pp. 3024–3030.
- [14] M. Swaminathan, F. S. Cabrera, J. S. Pujol, U. Muncuk, G. Schirner and K. R. Chowdhury, "Multi-Path Model and Sensitivity Analysis for Galvanic Coupled Intra-Body Communication Through Layered Tissue," in *IEEE Transactions on Biomedical Circuits and Systems*, vol. 10, no. 2, pp. 339–351, April 2016.
- [15] B. Kibret, M. Seyed, D. T. H. Lai and M. Faulkner, "Investigation of Galvanic-Coupled Intra-body Communication Using the Human Body Circuit Model," in *IEEE Journal of Biomedical and Health Informatics*, vol. 18, no. 4, pp. 1196–1206, July 2014.
- [16] M. A. Callejón, J. Reina-Tosina, D. Naranjo-Hernández and L. M. Roa, "Galvanic Coupling Transmission in Intra-body



- Communication: A Finite Element Approach,” in *IEEE Transactions on Biomedical Engineering*, vol. 61, no. 3, pp. 775–783, March 2014.
- [17] M. A. Callejón, D. Naranjo-Hernández, J. Reina-Tosina and L. M. Roa, “A Comprehensive Study into Intrabody Communication Measurements,” in *IEEE Transactions on Instrumentation and Measurement*, vol. 62, no. 9, pp. 2446–2455, Sept. 2013.
- [18] M. A. Callejón, D. Naranjo-Hernandez, J. Reina-Tosina and L. M. Roa, “Distributed Circuit Modeling of Galvanic and Capacitive Coupling for Intrabody Communication,” in *IEEE Transactions on Biomedical Engineering*, vol. 59, no. 11, pp. 3263–3269, Nov. 2012.
- [19] M. D. Pereira, G. A. Alvarez-Botero and F. Rangel de Sousa, “Characterization and Modeling of the Capacitive HBC Channel,” in *IEEE Transactions on Instrumentation and Measurement*, vol. 64, no. 10, pp. 2626–2635, Oct. 2015.
- [20] Ž. Lucev, I. Krois and M. Cifrek, “A Capacitive Intrabody Communication Channel from 100 kHz to 100 MHz,” in *IEEE Transactions on Instrumentation and Measurement*, vol. 61, no. 12, pp. 3280–3289, Dec. 2012.
- [21] K. Zhao, Z. Ying and S. He, “Intrabody Communications Between Mobile Device and Wearable Device at 26 MHz,” in *IEEE Antennas and Wireless Propagation Letters*, vol. 16, pp. 1875–1878, 2017.
- [22] M. I. Kazim, M. I. Kazim and J. J. Wikner, “Realistic path loss estimation for capacitive body-coupled communication,” *2015 European Conference on Circuit Theory and Design (ECCTD)*, Trondheim, 2015, pp. 1–4.
- [23] J. Wang, Y. Nishikawa and T. Shibata, “Analysis of On-Body Transmission Mechanism and Characteristic Based on an Electromagnetic Field Approach,” in *IEEE Transactions on Microwave Theory and Techniques*, vol. 57, no. 10, pp. 2464–2470, Oct. 2009.
- [24] K. Sayrafian-Pour, W. B. Yang, J. Hagedorn, J. Terrill and K. Y. Yazdandoost, “A statistical path loss model for medical implant communication channels,” *2009 IEEE 20th International Symposium on Personal, Indoor and Mobile Radio Communications*, Tokyo, 2009, pp. 2995–2999.
- [25] T. S. P. See, X. Qing, Z. N. Chen, C. K. Goh and T. M. Chiam, “RF transmission in/through the human body at 915 MHz,” *2010 IEEE Antennas and Propagation Society International Symposium*, Toronto, ON, 2010, pp. 1–4.
- [26] D. Werber, A. Schwentner and E. M. Biebl, “Investigation of RF transmission properties of human tissues,” in *Advances in Radio Science*, vol. 4, pp. 357–360, 2006.
- [27] J. N. Bringuier and M. Raj, “Electromagnetic Wave Propagation in Body Area Networks Using the Finite-Difference-Time-Domain Method,” in *Sensors*, vol. 12, no. 7, pp. 9862–9883, 2012.
- [28] T. S. P. See and Z. N. Chen, “Experimental Characterization of UWB Antennas for On-Body Communications,” in *IEEE Transactions on Antennas and Propagation*, vol. 57, no. 4, pp. 866–874, April 2009.
- [29] P. Soontornpipit, C. M. Furse and You Chung Chung, “Design of implantable microstrip antenna for communication with medical implants,” in *IEEE Transactions on Microwave Theory and Techniques*, vol. 52, no. 8, pp. 1944–1951, Aug. 2004.
- [30] M. Seyedi, B. Kibret, D. T. H. Lai and M. Faulkner, “A Survey on Intrabody Communications for Body Area Network Applications,” in *IEEE Transactions on Biomedical Engineering*, vol. 60, no. 8, pp. 2067–2079, Aug. 2013.
- [31] A. S. Y. Poon, S. O’Driscoll and T. H. Meng, “Optimal Frequency for Wireless Power Transmission into Dispersive Tissue,” in *IEEE Transactions on Antennas and Propagation*, vol. 58, no. 5, pp. 1739–1750, May 2010.
- [32] N. B. Asan *et al.*, “Intra-body microwave communication through adipose tissue,” in *Healthcare Technology Letters*, vol. 4, no. 4, pp. 115–121, Aug. 2017.
- [33] N. B. Asan *et al.*, “Human fat tissue: A microwave communication channel,” *2017 First IEEE MTT-S International Microwave Bio Conference (IMBIOC)*, Gothenburg, 2017, pp. 1–4.
- [34] E. Hassan, D. Noreland, E. Wadbro and M. Berggren “Topology Optimisation of Wideband Coaxial-to-Waveguide Transitions,” *Scientific Reports* 7, 45110, Mar. 2017. doi: 10.1038/srep45110.
- [35] Keysight Technologies. 8507E Dielectric probe kit. Available at <http://www.keysight.com/en/pd-304506-pn-85070E/dielectric-probe-kit?cc=SE&lc=eng>, accessed July 2017.
- [36] S. Gabriel, R. W. Lau, C. Gabriel, “The dielectric properties of biological tissues: II. Measurements in the frequency range 10 Hz to 20 GHz,” *Physics in Medicine & Biology*, vol. 41, pp. 225–2269, 1996.
- [37] IEEE Standard for Local and metropolitan area networks—Part 15.4: Low-Rate Wireless Personal Area Networks (LR-WPANs), in *IEEE Std 802.15.4-2011 (Revision of IEEE Std 802.15.4-2006)*, pp. 1–314, Sept. 2011.
- [38] H. Simon and M. Michael, “Passband Digital Transmission,” in *Communication Systems*, 4<sup>th</sup> ed. New York: Wiley, 2001, ch. 6, sec. 3, pp 361–362.
- [39] B. Bloessl, C. Leitner, F. Dressler, and C. Sommer, “A GNU Radio-based IEEE 802.15.4 Testbed,” in *12. GI/ITG KuVS Fachgespräch Drahtlose Sensornetze (FGSN 2013)*, pp. 37–40, Cottbus, Germany, September 2013.
- [40] Keysight Technologies. N9918A fieldfox handheld microwave analyzer, 26.5 GHz. <http://www.keysight.com/en/pdx-x201927-pn-N9918A/fieldfox-handheld-microwave-analyzer-265-ghz?nid=32495.1150498&cc=SE&lc=eng>, accessed July 2017.
- [41] D. Kurup, W. Joseph, G. Vermeeren and L. Martens, “In-body Path Loss Model for Homogeneous Human Tissues,” in *IEEE Transactions on Electromagnetic Compatibility*, vol. 54, no. 3, pp. 556–564, June 2012.
- [42] S. Misra, S. C. Misra, I. Woungang, “Transmission Power Control for Mobile Ad Hoc Networks”, in *Selected Topics in Communication Networks and Distributed Systems*, Singapore: World Scientific, 2010, ch. 7, pp. 193–216.



**Noor Badariah Asan** was born in Malaysia, in 1984. She received the B.E. degree in Electronic Engineering from Universiti Teknikal Malaysia Melaka, Malaysia, in 2008, and the M.E. degree in communication and computer from National University of Malaysia, Selangor, Malaysia, in 2012. In 2010, she joined the Department of Electronic and Computer Engineering, Universiti Teknikal Malaysia Melaka, as a Lecturer. She is currently a PhD student in the Department of Engineering Sciences, Uppsala University, since 2015. Her current research interests include intra-body communication, wireless sensor network and designing biomedical sensor.



**Carlos Pérez-Penichet** got his degree in Physics from the University of Havana, Cuba in 2009. Since 2011 he is dedicated to the study of communication engineering. His main interests are low-power wireless networks and the internet of things. He is currently a PhD student at Uppsala University in Sweden.



**Syaiful Redzwan Mohd Shah** was born in Malaysia, in 1984. He received the B.E. degree in Electronic Engineering (Telecommunication Electronics) and the M.Sc. degree in communication and computer from Universiti Teknikal Malaysia Melaka, Malaysia, in 2007 and 2010, respectively. In between 2011 to 2013, he was working as a Research Engineer at Huawei Technologies, Malaysia. He was with the LG CNS Ltd., Malaysia, as a senior research engineer from 2013 to 2015. He is currently a PhD student in the Department of Engineering Sciences, Uppsala University, since 2015. His research interest includes designing of BMD sensors, microwave material characterization, non-invasive diagnostics and biomedical sensors.



**Daniel Noreland** is a researcher in scientific computing at Umeå University, Sweden. He received his M.Sc. in Engineering physics in 1998 and his Ph.D. in numerical analysis from Uppsala University in 2003. His current research interest is mainly directed toward shape and topology optimization in acoustics and electromagnetics.



**Taco Blokhuis** is a trauma surgeon. After finishing his study in Medicine in Amsterdam in 1996 he obtained his PhD in 2001. After finishing his training as a trauma surgeon, he has been working in university medical centers throughout the Netherlands. In 2014, he was appointed as Associate Professor at the University of Utrecht. He is currently working in the Maastricht University Medical Center. Besides his clinical tasks his focus is on basic (pre-clinical) research.



**Emadelddeen Hassan** received the B.S. and M.S. degrees in electronics and communication engineering from Menoufia University, Egypt, in 2001 and 2006, and the Licentiate and Ph.D. degrees in computational science and engineering from Umeå University, Umeå, Sweden in 2013 and 2015, respectively.

His research interests include numerical methods in EM, Antenna design optimization, EBG, defected ground structures, non-destructive evaluation and

testing, optimization methods, and parallel programming.



**Thiemo Voigt** is Professor of Computer Science at the Department of Information Technology at Uppsala University, Sweden. He also leads the Networked Embedded Systems group at RISE SICS. He received his Ph.D. in 2002 from Uppsala University. His current research focuses on system software for embedded networked devices and the Internet of Things. Prof. Voigt's work has been cited more than 9000 times. He is a member of the editorial board for the IEEE Internet of Things and ACM Transactions on

Sensor Networks (TOSN).



**Anders Rydberg** became member of IEEE 1989. He received the M.Sc.-degree from Lund University of Technology in 1976. In 1988 and 1991, he received the Ph.D. degree and was appointed Docent (Associated Professor) respectively, at Chalmers University of Technology. In 1992, he was employed as Senior Lecturer and in 2001 as Professor in Applied Microwave and Millimeter-wave Technology at Uppsala University. He is heading the Microwave Group at the Department of Engineering Science, Uppsala

University. He worked between 1977 to 1983 at the National Defence Research Establishment, ELLEMTEL Development Co., and the Onsala Space Observatory. Between 1990 to 1991, he worked as a senior research engineer at Farran Technology Ltd., Ireland. He has authored or co-authored more than 250 publications in the area of EM-bio interaction, micro- and millimeter-wave antennas, sensors, solid state components and circuits and has three patents in the areas. He has graduated seven Ph.D. students.

Prof. Rydberg is a member of the editorial board for the IEEE-MTT, Chairman for Section D of the Swedish Member Committee of URSI (SNRV), and member of the board for the Swedish IEEE MTT/AP Chapter.



**Robin Augustine**, graduated in Electronics Science from Mahatma Gandhi University, India in 2003. He received Master's degree in Electronics from Cochin University of Science and Technology, Cochin, India in 2005. Received PhD in Electronics and Optronics Systems from Université de Paris Est Marne La Vallée, France in July 2009. He was the recipient of UGCRFSMS fellowship for meritorious students from Indian government and EGIDE Eiffel grant for excellence from French research ministry in

2006 and 2008 respectively. He worked at Université de Paris Est and University of Rennes 1, IETR as Post Doc from 2009 to 2011. Since 2011 he is working as senior researcher at Uppsala University. In February 2016, he was appointed Docent (Associate Professor) in Microwave Technology at Uppsala University. He is the Swedish PI of the Eureka Eurostars project COMFORT and Indo-Swedish Vinnova-DST funded project BDAS. He is leading the Microwaves in Medical Engineering Group (MMG) at Solid State Electronics Division, Uppsala University. He is author or co-author of more than 70 publications including journals and conferences in the field of sensors, microwave antennas, bio-electromagnetics and material characterization. Dr. Augustine is a member of the editorial board for the IET Electronics letters and Medical Research and Innovation Journal. His current research field includes designing of wearable antennas, BMD Sensors, Dielectric characterization, Intra-Body Area Networks, Bioelectromagnetism, Non-invasive Diagnostics, biological healing effects of RF in in-vitro and in-vivo systems.